ISSN 0001-4338, Izvestiya, Atmospheric and Oceanic Physics, 2022, Vol. 58, No. 9, pp. 1150–1159. © Pleiades Publishing, Ltd., 2022.
Russian Text © The Author(s), 2022, published in Issledovanie Zemli iz Kosmosa, 2022, No. 1, pp. 68–79.

PHYSICAL BASES OF STUDYING THE EARTH FROM SPACE

Evaluation of Some Parameters of the Topsoil from Radar and Optical Data of Sentinel 1/2 Satellites Using the Example of the Novosibirsk Region

N. V. Rodionova[a], *, S. Ya. Kudryashova[b], and A. S. Chumbaev[b]

[a] *Kotel'nikov Institute of Radioengineering and Electronics, Russian Academy of Sciences, Fryazino Department, Fryazino, Moscow oblast, 141190 Russia*

[b] *Institute of Soil Science and Agrochemistry, Siberian Branch, Russian Academy of Sciences, Novosibirsk, 630090 Russia*

**e-mail: rnv@ire.rssi.ru*

Received December 3, 2020

Abstract—This paper considers the use of radar and optical data from the Sentinel 1 and Sentinel 2 satellites for 2019–2020 to assess the humus content and the percentage of clay and moisture in the topsoil using the example of chernozems and gray forest soils of the Novosibirsk oblast. Particular attention is paid to the selection of satellite images, because in order to quantify the humus content and clay in the soil, it is necessary to fulfill the conditions for the soil to be dry and bare. The humus content is estimated for five test sites based on a regression model (Karavanova and Orlov, 1996), which includes surface reflection coefficients at the wavelength of the B6 spectral channel of the Sentinel 2 satellite. The model parameters are adjusted for the conditions of the study area separately for chernozems and gray forest soils. The percentage of physical clay in the soil is estimated using Sentinel 2 optical data, ground measurements, and regression models with an exponential dependence of clay content on soil reflectances at the SWIR wavelengths of the Sentinel 2 spectral channels (Bousbih et al., 2019; Shabou et al., 2015). The change in the percentage of humus and clay content in the test sites of soils over the year is shown according to Sentinel 2 data. The topsoil moisture content is estimated based on radar, optical, and the combined use of radar and optical data.

Keywords: C-band radar data, backscatter factor, optical data, reflectance, soil humus content, soil clay content, soil moisture

DOI: 10.1134/S0001433822090195

INTRODUCTION

Soil optical properties are mainly affected by four important factors: mineral composition, soil moisture, organic matter content, and soil texture. For the remote reconstruction of these parameters, different groups of spectral indices are used. Radar data provide information on soil surface roughness and dielectric permittivity depending on soil moisture and texture (physical clay and physical sand content).

In this paper, we consider the possibility of using radar data from the Sentinel 1 (S1) satellite and optical data from the Sentinel 2 (S2) satellite for 2019–2020 to estimate the content of moisture, humus (H), and clay (Clay) in the topsoil (0–10 cm) using the example of chernozems and gray forest soils of Novosibirsk oblast. Particular attention is paid to the selection of satellite images, since for such an assessment there are certain requirements for the soil; namely, the soil must be dry and without vegetation.

STUDY AREA DESCRIPTION

The object of study is the soils of six test sites located in Novosibirsk oblast. From October 8 to 11, 2019, on the territory of the test sites (Fig. 1), temperature sensors were installed on not washed-off (unwashed) chernozems (arable land), slightly washed away (arable land), virgin land and gray forest soils not washed away (arable land), slightly washed away (arable land), forest. Sensors are installed to fix the air temperature (at a height of 2 m) and the temperature at the depths of the soil profile: on the soil surface, 0 cm, and at a depths of 5, 10, 15, 20, 40, 60, 80, 100, 120, 140, and 160 cm. The measurement interval is 3 h; the measurements started on October 10. Soil samples were taken to determine their basic physical and chemical properties.

Figure 1 (top) shows the location of the test sites (highlighted by a red rectangle) at a distance of about 55 km east of Novosibirsk. The image was obtained according to Sentinel 2 data on April 23, 2019, in nat-

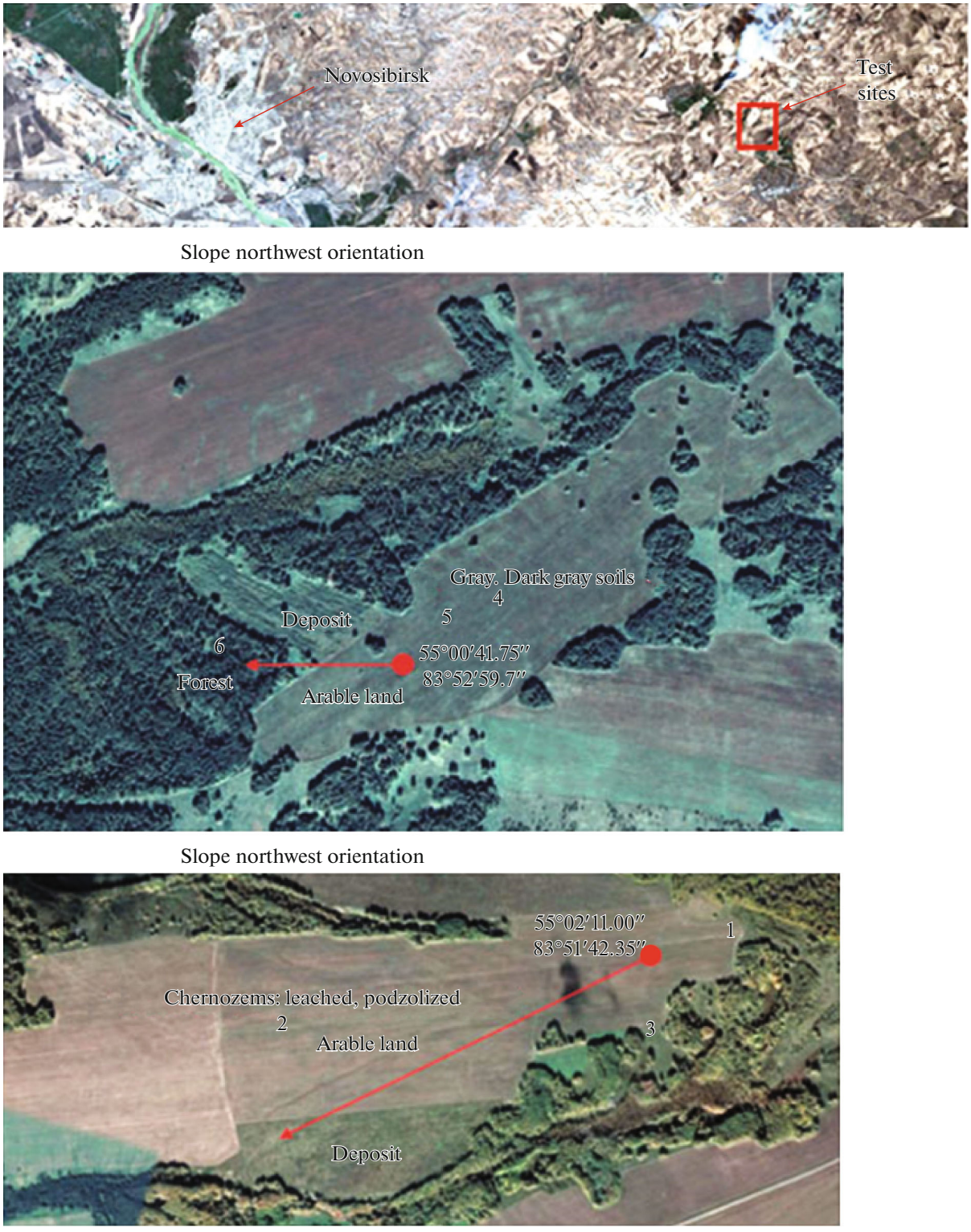

Fig. 1. Test sites in the Novosibirsk oblast.

ural colors (combination of channels B4–B3–B2). Figure 1 (bottom) shows a detailed map of the location of chernozems (slope southwest orientation) and gray forest soils (slope northwest orientation) on test sites with test site numbers.

Table 1 gives the coordinates of the test sites, as well as the measured values of the percentage of humus and the particle size distribution of soil samples at a depth of 0–10 cm (2019 data) (GOST 26213-91 Soils. Methods for Determining Organic Matter and

Table 1. Description of test sites in Novosibirsk oblast

Site	N, E coordinates	Soil particle size distribution and humus content, %			
		Clay	Sand	Silt	Humus
1. Chernozem leached, arable land not washed off	55°02′12.3″, 83°51′47.8″	25.6	53.7	20.7	9.9
2. Chernozem leached, arable land slightly washed away	55°01′42.8″, 83°50′41.8″	19.8	56.8	23.4	8.3
3. Chernozem leached, slightly washed away virgin land	55°01′55.4″, 83°51′29.6″	22.1	51.8	26.1	8.6
4. Gray forest soil, arable land not washed off	55°00′42.0″, 83°53′01.1″	22.9	54.8	22.3	6.0
5. Gray forest soil, arable land slightly washed away	55°00′40.5″, 83°52′54.1″	24.4	55.1	20.5	5.2
6. Gray forest soil, forest	55°00′37.8″, 83°52′31.8″	25.0	54.2	20.8	6.6

Table 2. Spearman correlation coefficient ρS between BSC and air and soil temperatures

Site	BSC	T°, air	T°, soil surface	T°, soil 5 cm
2. Chernozem leached, arable land slightly washed away	σ^0_{VV}	$\rho_S = 0.46$, $p = 0.03$	$\rho_S = 0.36$, $p = 0.07$	$\rho_S = 0.15$, $p = 0.27$
	σ^0_{VH}	$\rho_S = 0.47$, $p = 0.02$	$\rho_S = 0.28$, $p = 0.12$	$\rho_S = 0.32$, $p = 0.01$
3. Chernozem leached, slightly washed away virgin land	σ^0_{VV}	$\rho_S = 0.69$, $p = 0.0005$	$\rho_S = 0.41$, $p = 0.04$	$\rho_S = 0.61$, $p = 0.003$
	σ^0_{VH}	$\rho_S = 0.81$, $p = 0.00002$	$\rho_S = 0.44$, $p = 0.03$	$\rho_S = 0.6$, $p = 0.004$

GOST 12536-2014 Soils. Methods of Laboratory Granulometric (Grain-Size) and Microaggregate Distribution).

USED DATA AND RESEARCH METHODS

Sentinel 1 Radar Data

The open-access Sentinel 1 radar data of the IW (interferometric wide swath) C-band mode with VV and VH polarizations and a spatial resolution of 10 m and a temporal resolution of 12 days were used in the work. The viewing angle is 42.66°–42.81°. The number of survey sessions considered is 18 from October 14, 2019, to May 5, 2020, which was determined by the time the temperature sensors were in the soil. S1 images were processed using the SNAP program (https://sentinel.esa.int/web/sentinel/toolboxes/sentinel-1). Data preprocessing included the selection of a fragment with the region of interest and radiometric calibration.

Figure 2 shows graphs of the change in the backscatter coefficient (BSC) for both polarizations for the period October 14, 2019, to May 5, 2020, for six test sites. Let us note the features of the behavior of the graphs: for cross-polarization, the differentiation of BSC values for different test sites is typical, namely, in descending order of BSC values: forest, virgin land, gray forest soils, chernozems. For co-polarization, the BSC maxima (forest) and BSC minima (chernozems) are preserved (except for 2–3 sessions out of 18), but there is no clear differentiation in the BSC values between gray forest soils and virgin lands.

The correlation of radar data with air temperature, soil surface temperature, and soil temperature at a depth of 5 cm is presented on the example of test sites 2 and 3 (Table 2, sample size $N = 18$).

It turned out that, for virgin land (site 3), the correlation is higher for all three cases. Let us construct a regression relation for the case with the highest Spearman's rank correlation coefficient $\rho_S = 0.81$ (virgin soil) between the BSC of cross-polarization and air temperature (Fig. 3a) and soil temperature at a depth of 5 cm (Fig. 3b).

Sentinel 2 Multispectral Data

The multispectral data of Sentinel 2 with high temporal, spatial, and spectral resolution were used in the work. The frequency of multispectral imaging by each satellite is 10 days, and when two satellites are in operation, it is 5 days. The multispectral camera has 13 channels with different spatial resolutions from 10

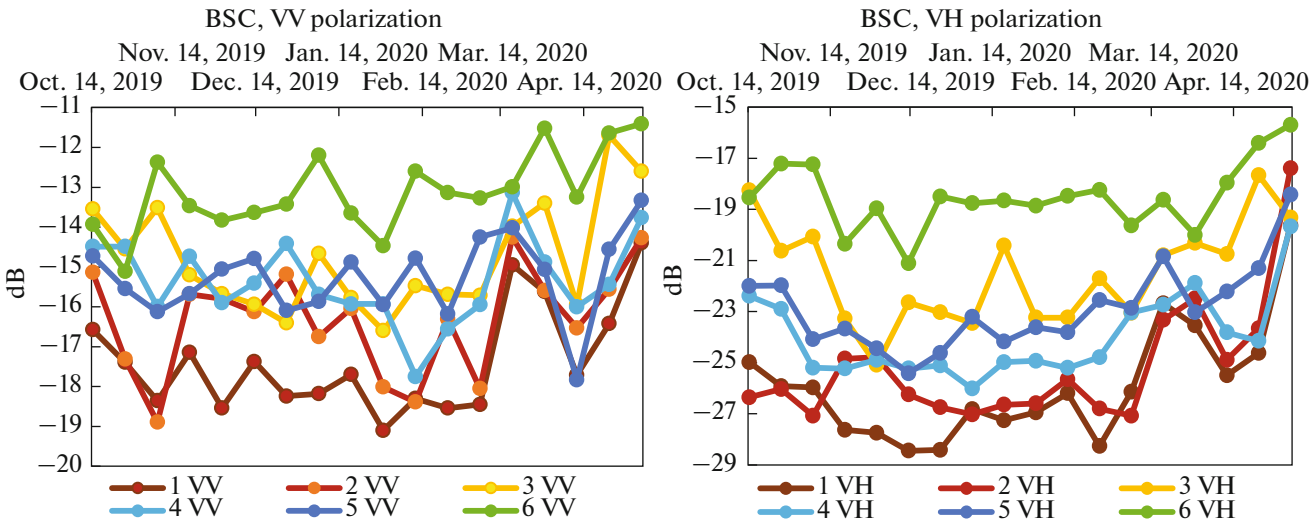

Fig. 2. Graphs of changes in the BSC for the period from October 14, 2019, to May 5, 2020, for test sites in Novosibirsk oblast.

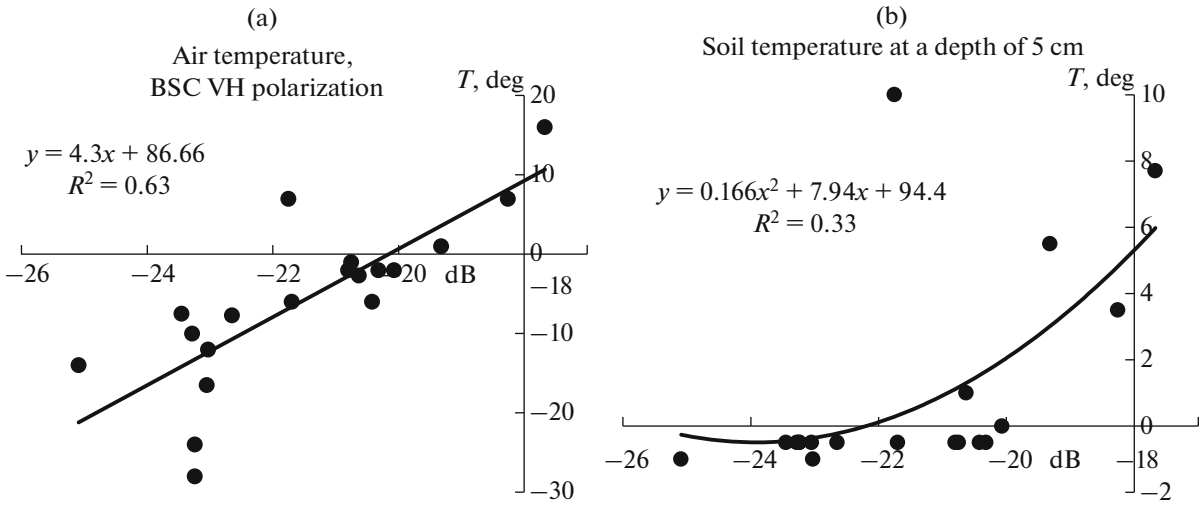

Fig. 3. Regression relationships between BSC (dB) and air temperature (a) and BSC and soil temperature at a depth of 5 cm (b) (site 3).

to 60 m. We used data from the S2 survey system with the processing level L2A in the form of albedo at the lower boundary of the atmosphere (with atmospheric correction). S2 images were processed by the SNAP program. Cloudless shooting sessions for April–May 2019 and 2020 were used.

Selection of S2 Source Images

For the satellite estimation of the content of organic matter and clay in the soil, restrictions are imposed on the choice of multispectral images associated with the identification of dry soils without vegetation (bare soils) in the images. The work (Dematte et al., 2018) gives conditions for S2 channels as follows (Castaldi et al., 2019): (1) zero cloudiness in the study area; (2) the vegetation index value NDVI = (B8 – B4)/(B8 + B4) < 0.35 to exclude green vegetation; (3) the difference in reflectance (CR) between channels B3 and B2 and channels B4 and B3 should be greater than 0 (the use of these filters improves soil identification (Dematte et al., 2018)); and (4) the value of NBR = (B11 – B12)/(B11 + B12) should be NBR ≤ 0.05, which makes it possible to distinguish pixels with dry bare soil in the image. Soil moisture enhances the absorption of light, and CR decreases sharply. The B11 and B12 spectral channels strongly correlate with soil moisture (Musick and Pelletier, 1988), and their difference makes it possible to distinguish the spectra of dry and wet soil, as well as the

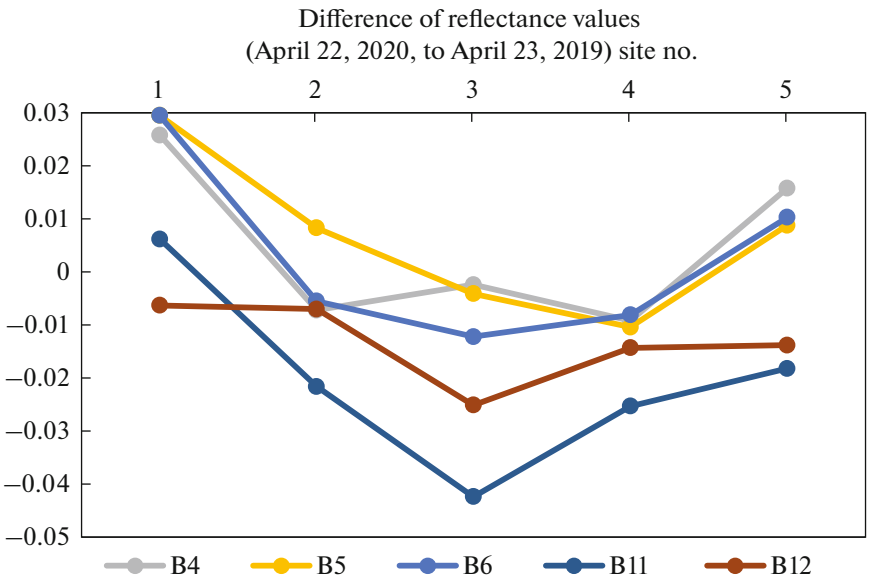

Fig. 4. Difference of reflectance values from the soils of the five test sites for the shooting sessions on April 22, 2020, and April 23, 2019.

spectra associated with vegetation. The choice of threshold for NBR greatly affects the number of pixels in the image that satisfy dry soil conditions. Increasing the NBR threshold to 0.15 leads to a twofold decrease in the number of "necessary" pixels (Castaldi et al., 2019); i.e., an increase in NBR leads to a deterioration in the accuracy of models for determining soil parameters from satellite data.

As a result, optical images S2 L2A for April 23, 2019, and April 22, 2020, were selected for the study area for which the condition of the absence of clouds is satisfied; NDVI varies from 0.17 to 0.24; the difference between the B3 and B2 channels and the B4 and B3 channels is greater than 0; and the values of NBR slightly exceed the threshold of 0.05—namely, NBR varies from 0.1 to 0.158. The given values are fulfilled for all sites, except for site 6 (forest), for which the value of NDVI > 0.5 and NBR > 0.17.

The Assessment of Humus Content in the Topsoil According to S2

The loss of soil organic carbon (SOC) is one of the main causes of arable land degradation. Thus, spatial and temporal monitoring of SOC is an extremely important task, the solution of which is the subject of numerous works (Orlov et al., 2001; Karavanova, Orlov, 1996; Castaldi et al., 2019; Gholizadeh et al., 2018; and many others). These authors obtained regression models with an exponential relationship between the SOC content and the reflectance (CR), and a different degree of negative correlation between the SOC content and the CR values depending on the spectral channel.

To create a regression model of the relationship between CR and (H), both satellite and ground data are needed, and the number of soil samples should be at least 20 to determine the correlation. In addition, the studied test areas should have a similar particle size distribution. The point is that the finer the soil particles are, the larger the CR from these soils (Karavanova, 2003). That is, the models for determining H are local, and the use of models available in the literature requires adjustment for the study area.

The works (Castaldi et al., 2019; Gholizadeh et al., 2018) show that the best correlation between the humus content in the soil and CR is observed in the spectral channels S2 B4–B6 and B11, B12. For a qualitative assessment of changes in the humus content in the soils of the test sites under study, we present the graphs of the difference between the values of the CR of the spectral channels S2 B4–B6, B11, and B12 for the shooting sessions on April 23, 2019, and April 22, 2020 (Fig. 4), for each test site, and evaluate the changes in the CR for a year.

Given the fact that the CR of these channels has a negative correlation with the humus content in the soil, we will estimate by the sign of the difference in which direction the change in the humus content occurred over the year. The difference in CR values is positive for site 1 (chernozem, not washed away arable land) for all channels, except for B12. This indicates that the CR values for site 1 increased in 2020 compared to 2019; i.e., the content of (H) decreased. For eroded chernozem (site 2), there is a decrease in the difference for four channels and an increase in the difference for one. For site 3 (virgin soil), the difference in CR for all channels is negative, which may indicate

Table 3. Parameters of the exponential equation and the percentage of humus determined from the equation in the soil of test sites in Novosibirsk oblast

Soils	Parameter values of the exponential equation			Site No.	H, % 2019	H, % 2020
	$\rho_{750,h}$	A	k			
Gray forest	8.5	40.5	0.28	4	6.0	6.4
				5	5.8	5.4
Chernozems: leached, ordinary, typical, meadow-chernozem soils	8.0	29.1	0.126	1	9.9	7.5
				2	6.8	7.1
				3	7.7	8.6

an increase in the content of (H). The situation is similar for site 4 (gray forest soils are not washed away). For weakly eroded gray soils (site 5), there is a positive difference for three channels and a negative difference for two.

To quantify (H), a local model for the test area is required, or the use of existing models with adjustments for a local area with its own soil granulometric composition.

Pokrovsky in 1927 was the first to propose an exponential equation that determines the relationship between humus content and CR values (according to Orlov et al., 2001):

$$\rho_{750} = \rho_{750,h} + Ae^{-k\mathrm{H}}. \quad (1)$$

where ρ_{750} is the CR at a wavelength of 750 nm, $\rho_{750,h}$ is the CR of a high-humus soil, $\rho_{750} = (\rho_{750,h} + A)$ is the CR of a humus-free soil, H is the humus content, and k is the coefficient that determines the steepness (slope) of the exponential graph.

When using the exponential dependence of CR on the humus content in dry bare soil, three points should be taken into account: (1) at a low humus content (up to 3%), its determination is the most accurate, but the spread in CR values corresponding to a given humus content is large; (2) at a humus content of 6–7% or more, the determination of the humus content by CR is inaccurate and the effect is exerted by soil moisture and processing conditions at the same humus content (Karavanova, 2003); and (3) the decisive factor is the choice of satellite imagery dates, which make it possible to identify pixels with dry bare soil.

In this work, it is not possible to find out the correlation between CR and humus content in five test sites of Novosibirsk oblast due to the insufficient number of ground measurement points. Judging by the available ground-based measurements of the humus content in the soils of the test sites (Table 1), we assume that the curves of the dependence of CR on (H) (humus) are represented by flattening areas, where the accuracy of determining the content of (H) from CR is low.

In this work, to determine the (H) content from satellite data, an exponential model with parameters for chernozems and gray forest soils presented in (Karavanova and Orlov, 1996) is used.

Note that, to match this model, we must take the optical data for a wavelength of 750 nm. For S2, this is the B6 channel with a wavelength of 740 nm, a bandwidth of 15 nm, and a spatial resolution of 20 m. To use the parameters of the exponential equation according to (Karavanova, Orlov, 1996) in the local conditions of the studied test areas, it is necessary to correct these parameters. One possible option for assessing the humus content in the soils of the test sites is to use the following parameters for chernozems: $\rho_{750,h} = 8.0$, $A = 29.1$, and $k = 0.1256$. For gray forest soils, $\rho_{750,h} = 8.5$, $A = 40.5$, and $k = 0.28$. Table 3 shows the calculated values of the humus content (H) for five test sites with the given coefficients of the exponential equation.

The difference between the obtained values of the percentage of humus (H) according to the equation (Table 3) and the values obtained in laboratory conditions (Table 1) is no more than 1.5% in absolute value for 2019. The sources of errors lie primarily in the insufficient amount of ground data. For each type of soil (chernozems and gray forest soils), about 20 or more ground measurements are required, one part of which is used to obtain the exponential parameters and the second part is used to validate the resulting equation. The more such ground data, the more reliable the formula. The second point that leads to errors is the choice of the initial optical image, for which the most important parameter is the value of the NBR spectral index. Increasing the value of NBR > 0.05 significantly reduces the number of pixels that satisfy the condition of dry bare soil. Nevertheless, some conclusions about the quantitative content of humus in the soil can be drawn, first and foremost, about the change in H values over the year (2019–2020). The greatest difference was obtained for site 1: a decrease in the humus content by 2.4% per year. For other sites, changes over the year are insignificant, from 0.3 to 0.9% (see Table 3).

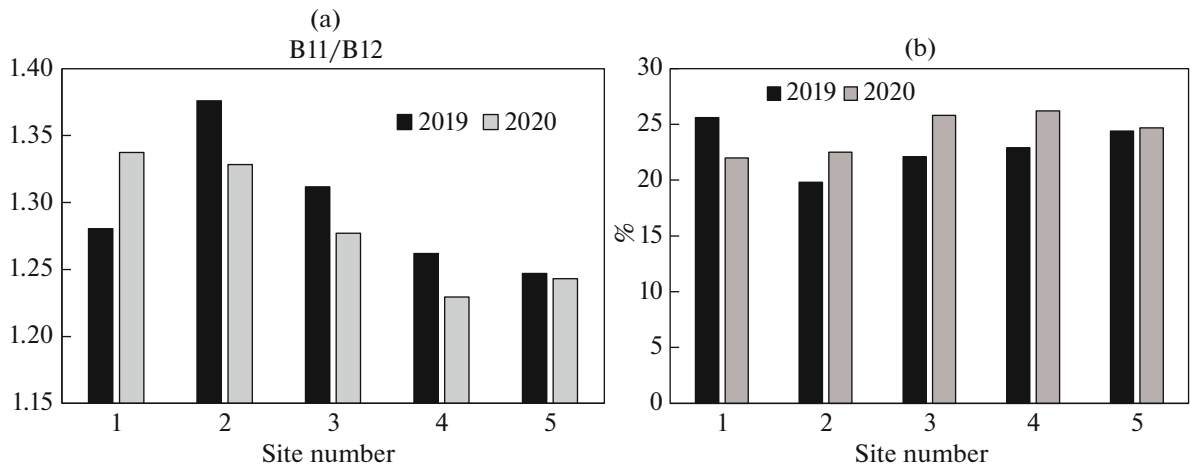

Fig. 5. Qualitative assessment of changes in the values of the clay index CI for the year (a) and quantitative assessment of changes in the values of the percentage of clay in the soils of the test sites (b).

Assessment of Clay Content in the Topsoil by S2 Satellite Optical Data

Numerous works are devoted to the assessment of soil texture components using remote optical data (Ukrainskiy and Chepelev, 2011; Shabou et al., 2015; Bousbih et al., 2019; Vaudouret al., 2019; Gholizadehet al., 2018; etc.). Thus, it was shown in (Gholizadehet al., 2018) that the best correlation with the clay content in the soil has the reflection coefficient of the B7 channel of the S2 satellite, as well as the spectral indices V = B8/B4 (Vegetation index), SAVI = 1.5(B8 – B4)/(B8 – B4 + 0.5) (Soil Adjusted Vegetation Index), and others. A weak correlation of S2 with silt and sand was noted. The authors (Bousbih et al., 2019) found that B11 (SWIR1) and B12 (SWIR2) S2 channels are the most sensitive to changes in the clay content in the soil and they have a negative correlation with this content. Moreover, for the use of these channels, the condition for obtaining a quantitative assessment of the clay content is dry bare soil. In (Hengl, 2007), the spectral clay index CI = B11/B12 (Clay Index) was introduced, which has a strong negative correlation with the clay content in the soil. It should be noted that the quantitative assessment of the content of clay in the soil is carried out locally for the study area, and the accuracy of the assessment is directly related to the number of test measurements of soil samples.

Figure 5a shows graphs of CI = B11/B12 values for two shooting sessions of S2 on April 23, 2019, and April 22, 2020, which makes it possible to make a qualitative comparison of annual changes in the clay content in the topsoil of test sites 1–5. Changes over the year in terms of clay content did not affect site 5; for sites 2–4 there is a slight increase in clay content, and there is a slight decrease for site 1.

A regression model (Castaldi et al., 2019) of the exponential relationship between the content of organic carbon in the soil and CR can become a quantitative estimate of the percentage of clay in the soil. For the case with clay, we use the clay index CI = B11/B12 as a variable in the exponent, which has a negative correlation with the content of clay in the soil. The formula for quantifying the percentage of clay in the soil is as follows: Clay(%) = 802exp(–2.69CI) for chernozems; Clay(%) = 5123.6exp(–4.29CI) for gray forest soils. Part of the ground-based measurements of the clay content in the soil of the test sites of the Novosibirsk region was used to obtain the exponential parameters, and the rest was used for validation. The resulting formulas are of a local nature, and the accuracy of the coefficients in them directly depends on the number of ground-based measurements.

Checking for a correlation of CI with soil texture elements showed that there is no negative correlation of CI with silt and physical clay. In the Clay formulas, these are particles with a diameter greater than 0.001 mm and less than 0.01 mm.

Figure 5b shows graphs of the percentage of clay in the soils of five test sites (measured values) and calculated using the formulas above for 2020.

The qualitative assessment of the clay content in the soils of the test sites by the value of the clay index does not contradict the quantitative assessment by the regression model.

Topsoil Moisture Estimation Using Optical and Radar Data S1 and S2

Let us consider the possibility of estimating the soil moisture from optical data, radar data, or the joint use of optical and radar data.

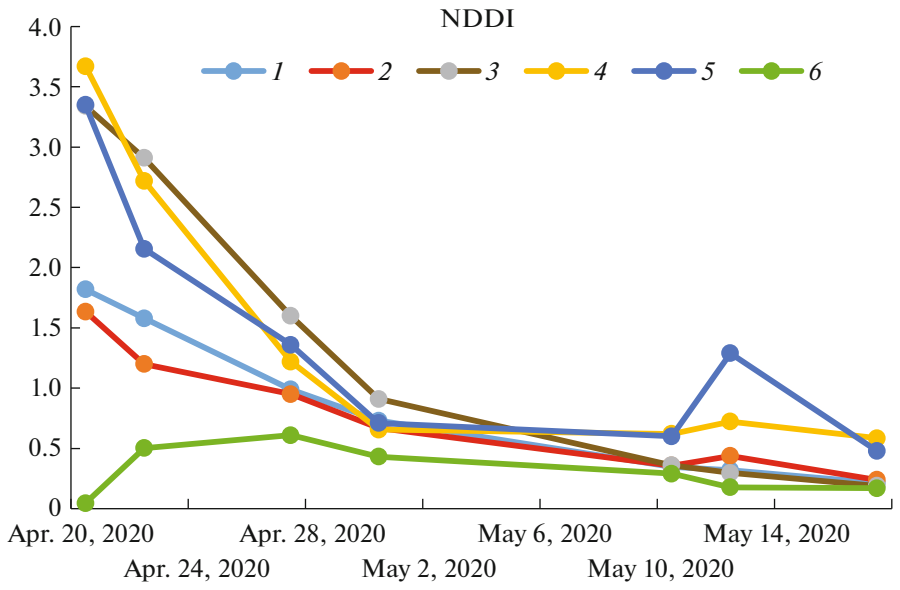

Fig. 6. NDDI plots for the studied sites with chernozems and gray forest soils for April and May 2020.

Optical Data

The work (Burapapol and Nagasawa, 2016) uses the NDDI index (normalized difference drought index) to assess soil moisture:

$$\mathrm{NDDI} = \frac{\mathrm{NDVI} - \mathrm{NDWI}}{\mathrm{NDVI} + \mathrm{NDWI}}, \qquad (2)$$

where $\mathrm{NDWI} = \frac{\mathrm{B8A} - \mathrm{Bl1}}{\mathrm{B8A} + \mathrm{Bl1}}$ or $\mathrm{NDWI} = \frac{\mathrm{B8A} - \mathrm{Bl2}}{\mathrm{B8A} + \mathrm{Bl2}}$ (normalized difference wet index), B8A, B11, and B12 are S2 spectral channels. The authors showed that higher NDDI values correspond to lower soil moisture values. In this work, the B12 channel was used to calculate NDWI. The NDDI plot for the studied sites with chernozems (sites 1, 2, and 3 (virgin lands)) and gray forest soils (4, 5, and 6 (forest)) is shown in Fig. 6 for optical shooting sessions for April (20, 27, and 30) and May (10, 12, and 17) 2020.

A strong differentiation of NDDI values for different sites for the survey session on April 20, 2020, and a grouping of test sites according to close soil moisture values were revealed. The soil of site 6 (forest) has the highest humidity. Sites 4, 5 (gray forest soils, arable land), and 3 (chernozems, virgin lands) are distinguished by the lowest humidity. Areas 1 and 2 are grouped between these extreme values (chernozems that are not washed away and washed away, arable land). In the transition from April to May, the differentiation of sites in terms of NDDE values decreases significantly, leading to the closeness of soil moisture values for all test sites.

Radar Data

The paper (Baghdadi et al., 2016) proposed a semiempirical model for determining the moisture content of bare soil based on the Dubois model (Dubois et al., 1995). The model parameters were obtained on the basis of a large number of measurements for X, C, and L sensors in the wavelength ranges with viewing angles of 20°–45°. The authors (Baghdadi et al., 2016) demonstrate a more accurate assessment of soil moisture. Here are the formulas of this model for the VV and VH polarizations, which correspond to the polarizations of the IW GRD Sentinel 1 mode:

$$\sigma^0_{\mathrm{VV}} = 10^{-1.138}(\cos\theta)^{1.528}\,10^{0.008c\tan(\theta)mv}\,f(h)^{0.71\sin(\theta)}, \qquad (3)$$

$$\sigma^0_{\mathrm{VH}} = 10^{-2.325}(\cos\theta)^{-0.01}\,10^{0.011c\tan(\theta)mv}\,f(h)^{0.44\sin(\theta)}, \qquad (4)$$

where σ^0_{VV} and σ^0_{VH} are the backscatter coefficient for the VV and VH polarizations, θ is the viewing angle, m_v is the volumetric soil moisture in %, and $f(h)$ is a function of soil surface roughness. Recall that, for the applicability of the Dubois model (Dubois et al., 1995), a number of conditions must be met, namely, the surface roughness $kh \le 2.5$, $mv \le 35\%$, $\theta \ge 30°$, and $k = 2\pi/\lambda$.

From formulas (3) and (4) to determine m_v, we obtain the following expression:

$$m_v = (\log_{10} A - \log_{10} B)/C, \qquad (5)$$

where

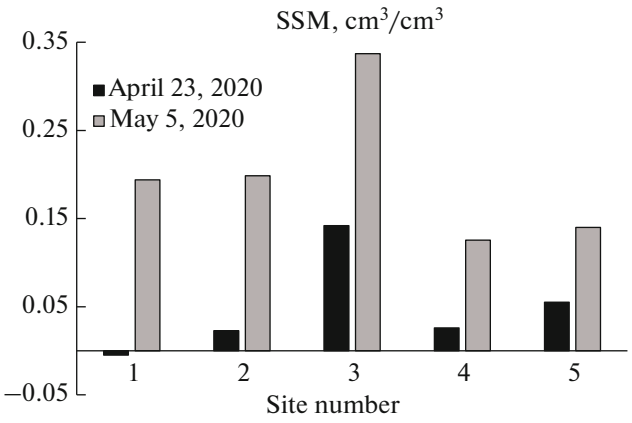

Fig. 7. Graphs of SSM changes (cm^3/cm^3) for two adjacent dates of the radar survey on April 23 and May 5, 2020.

$$A = 10^{1.15}(\cos\theta)^{0.6794},$$
$$B = (\sigma^0_{VV})^{0.44}/(\sigma^0_{VH})^{0.71}, \quad (6)$$
$$C = 0.00429\cot\theta.$$

For a viewing angle of 43°, the value is $A = 11.4204$ ($\log 10A = 1.05768$), $C = 0.0046$.

Only $m_v \le 35\%$ can be used from the obtained numerical values of soil moisture.

Sharing of Radar and Optical Data

The authors (Bao et al., 2018) proposed a new method for restoring surface soil moisture (SSM) under partially vegetated conditions based on the combined use of Sentinel 1 radar data and Landsat 8 OLI optical data and a water cloud model. The authors show that (1) for a vegetated surface, NDWI = (B8A – B11)/(B8A + B11) is most suitable for eliminating the influence of vegetation in estimating soil moisture; (2) Sentinel 1 VV polarization data is more suitable for SSM reconstruction in comparison with HV polarization, including due to higher accuracy; (3) the model allows obtaining SSM with high accuracy, as is evidenced by the correlation coefficient $R = 0.911$ with a root-mean-square error of 0.053 cm^3/cm^3 between the measured SSM and that obtained by the model. Given provisions (1)–(3), the formula for determining the volumetric soil moisture SSM in a layer of 0–5 cm is as follows:

$$\begin{aligned} SSM &= 0.539 + 0.044\sigma^0_{VV} + \sigma^0_{VV}\sec\theta \\ &\times \left(-0.008 + 0.016NDWI + 0.031NDWI^2\right) \\ &+ NDWI(0.444 + 2.964NDWI \\ &+ 11.15NDWI^2 - 33.75NDWI^3), \end{aligned} \quad (7)$$

where SSM is measured in cm^3/cm^3 and σ^0_{VV} in dB. It should be noted (Bao et al., 2018) that model (7) ignores the effect of surface roughness and vegetation type.

In this work, to calculate NDWI in (7), we used the B12 channel, as above when calculating NDDI. To calculate the SSM, we used radar data for April 23 and May 5, 2020, and optical data for April 22 and May 10, 2020, respectively, in the latter case, due to the lack of cloudless sessions from April 30 to May 10. Figure 7 shows plots of SSM (cm^3/cm^3) for two adjacent dates of the radar survey on April 23 and May 5, 2020. Note the negative SSM value for site 1, which is a consequence of the limited accuracy of the model (Bao et al., 2018).

The estimates of the moisture content of the topsoil, both qualitative from optical data (Fig. 6) and quantitative from radar data (given the values not exceeding 35%), and the combined use of radar and optical data (Fig. 7), showed their consistency, general trends, and the ability to compare the degree of moisture in the topsoil for different sites remotely in the absence of ground measurements.

CONCLUSIONS

This paper considers the use of radar and optical data from the Sentinel 1 and Sentinel 2 satellites for 2019–2020 to assess the humus content and the percentage of clay and moisture in the topsoil using the example of chernozems and gray forest soils of Novosibirsk oblast. Based on the readings of temperature sensors installed at the test sites and Sentinel 1 satellite data, the presence of a positive correlation of the BSC with the values of air temperature, soil surface temperature, and soil temperature at a depth of 5 cm with a Spearman correlation coefficient, respectively, of 0.8, 0.44, and 0.6 for VH polarization and 0.69, 0.41, and 0.6 for VV polarization (site 3), was shown.

An estimate of the moisture content of the topsoil of the test sites was made on the basis of radar and optical data, as well as on the basis of their joint use based on existing models.

A qualitative and quantitative assessment of the annual change in the content of humus and clay in the topsoil of the test sites based on Sentinel 2 multispectral data and regression models showed the largest change in the percentage of humus and clay for site 1 (leached chernozem, arable land not washed away), namely, a decrease in the percentage of humus by 2.4% and clay by 3.6%. For the rest of the sites, the change over the year in the percentage of humus in comparison with site 1 is insignificant, and clay is slightly increased in 2020 when compared with 2019. It was not possible to compare the changes over the year in the percentage of humus and clay in the soils of the test sites according to remote sensing data with ground measurements because field work was suspended in 2020 due to the pandemic.

FUNDING

This work was carried out as part of State Task on the topic 0030-2019-0008 Space, as well as State Task of the Institute of Soil Science and Agrochemistry, Siberian Branch, Russian Academy of Sciences.

CONFLICT OF INTERESTS

The authors declare that they have no conflicts of interest.

REFERENCES

Baghdadi, N., Choker, M., Zribi, M., El Hajj, M., Paloscia, S., Verhoest, N.E.C., Lievens, H., Baup, F., and Mattia, F., A new empirical model for radar scattering from bare soil surfaces, *Remote Sens.*, 2016, vol. 8, no.11, p. 920. https//doi.org/doi:10.3390/rs8110920.

Bao, Y., Lin, L., Wu, Sh., Deng, Kh.A.K., and Petropoulos, G.P., Surface soil moisture retrievals over partially vegetated areas from the synergy of Sentinel-1 and Landsat 8 data using a modified water-cloud model, *Int. J. Appl. Earth Obs. Geoinf.*, 2018, vol. 72, pp. 76–85.

Bousbih, S., Zribi, M., Pelletier, Ch., Gorrab, A., Lili-Chabaane, Z., Baghdadi, N., Ben Aissa, N., and Mougenot, B., Soil texture estimation using radar and optical data from Sentinel-1 and Sentinel-2, *Remote Sens.*, 2019, vol. 11, no. 13, p. 1520. https://doi.org/10.3390/rs11131520

Burapapol, K. and Nagasawa, R., Mapping soil moisture as an indicator of wildfire risk using Landsat 8 images in Sri Lanna National Park, Northern Thailand, *J. Agric. Sci.*, 2016, vol. 8, no. 10, pp. 107–119.

Castaldi, F., Chabrillat, S., Don, A., and van Wesemael, B., Soil organic carbon mapping using LUCAS topsoil database and Sentinel-2 data: An approach to reduce soil moisture and crop residue effects, *Remote Sens.*, 2019, vol. 11, no. 18, p. 2121. https://doi.org/10.3390/rs11182121

Demattê, J.A.M., Fongaro, C.T., Rizzo, R., and Safanelli, J.L., Geospatial Soil Sensing System (GEOS3): A powerful data mining procedure to retrieve soil spectral reflectance from satellite images, *Remote Sensing Environ.*, 2018, vol. 212, pp. 161–175.

Dubois, P.C., Van Zyl, J., and Engman, T., Measuring soil moisture with imaging radars, *IEEE Trans. Geosci. Remote Sens.*, 1995, vol. 33, no. 4, pp. 915–926.

Gholizadeh, A., Zizala, D., Saberioon, M., and Boruvka, L., Soil organic carbon and texture retrieving and mapping using proximal, airborne and Sentinel-2 spectral imaging, *Remote Sens. Environ.*, 2018, vol. 218, pp. 89–103.

Hengl, T., *A Practical Guide to Geostatistical Mapping of Environmental Variables*, Luxembourg: Office for Official Publications of the European Communities, 2007.

Kachinskii, N.A., *Mekhanicheskii i mikroagregatnyi sostav pochvy, metody ego izucheniya* (Mechanical and Microaggregate Composition of Soils and Methods for Its Analysis), Moscow: AN SSSR, 1958.

Karavanova, E.I., *Opticheskie svoistva pochv i ikh priroda* (Optical Properties of Soils and Their Nature), Moscow: MGU, 2003.

Karavanova, E.I. and Orlov, D.S., Estimate of the humus content in soils on the basis of their spectral reflectivity, *Agrokhimiya*, 1996, no. 1, pp. 3–9.

Musick, H.B. and Pelletier, R.E., Response to soil moisture of spectral indexes derived from bidirectional reflectance in thematic mapper wavebands, *Remote Sens. Environ.*, 1988, vol. 25, pp. 167–184.

Orlov, D.S., Sukhanova, N.I., and Rozanova, M.S., *Spektral'naya otrazhatel'naya sposobnost' pochv i ikh komponentov* (Spectral Reflectivity of Soils and Their Components), Moscow: MGU, 2001.

Shabou, M., Mougenot, B., Lili-Chabaane, Z., Walter, C., Boulet, G., Aissa, N., and Zribi, M., Soil clay content mapping using a time series of Landsat TM data in semi-arid lands, *Remote Sens.*, 2015, vol. 7, pp. 6059–6078.

Ukrainskii, P.A. and Chepelev, O.A., The granulometric composition of soils in the Oskol region according to interpreted space images, *Izv. Samar. Nauchn. Tsentra Ross. Akad. Nauk*, 2011, vol. 13, no. 1, pp. 1225–1229.

Vaudour, E., Gomez, C., Fouad, Y., and Lagacherie, P., Sentinel-2 image capacities to predict common topsoil properties of temperate and Mediterranean agroecosystems, *Remote Sens. Environ.*, 2019, vol. 223, pp. 21–33.

Translated by V. Selikhanovich